Penerbit Akademia Baru

Journal of Advanced Research Design

Journal homepage:
https://akademiabaru.com/submit/index.php/ard
ISSN: 2289-7984

Numerical Analysis and Experimental Validation of a Smart Wiper Washing System Prototype

Sharveswaran Ananthan[1], Roslina Mohammad[1,*], Nurazean Maarop[1], Shamsul Sarip[1], Mohamad Zaki Hassan[1], Mohamed Azlan Suhot[1], Sofian Bastuti[1,2], Rini Alfatiyah[2]

[1] Faculty of Artificial Intelligence, Universiti Teknologi Malaysia, Kuala Lumpur 54100, Malaysia
[2] Industrial Engineering, Pamulang University, Banten, Indonesia

ARTICLE INFO

Article history:
Received 16 September 2025
Received in revised form 19 October 2025
Accepted 26 October 2025
Available online 1 December 2025

Keywords:
Smart wiper system; finite element analysis; spray uniformity; prototype validation; automotive safety

ABSTRACT

Conventional windshield wiper washer systems often suffer from non-uniform spray coverage, leakage under pressure, and limited structural endurance, reducing their effectiveness in maintaining driver visibility during adverse weather conditions. This study addresses these challenges through the design, structural validation, and experimental testing of a smart wiper washing system prototype. The development process began with conceptual sketches and parametric modeling in SolidWorks, followed by finite element analysis in ANSYS using the von Mises stress criterion to evaluate structural integrity under internal pressurization. The perforated aluminum spray pipe demonstrated negligible deformation (<0.2 mm) and maximum stress values of ~2.25 MPa, well below the material yield strength, confirming a wide safety margin. A physical prototype was fabricated using locally available materials, integrating mechanical, fluidic, and electrical subsystems into a dual-mode actuation cycle: water spraying during the upward stroke and compressed air discharge during the downward stroke. Experimental validation showed spray uniformity above 85% and stable, repeatable wiper motion, with strong agreement between simulation predictions and measured performance. The findings confirm that the proposed system is both structurally robust and functionally reliable, offering a cost-effective and manufacturable solution for enhanced windscreen cleaning. This work contributes to automotive engineering by demonstrating how simulation-driven design can be translated into a validated prototype, providing a practical foundation for future refinement and durability studies.

1. Introduction

Automotive visibility in rainy or wet conditions remains a critical factor in road safety, as restricted visibility has been directly linked to higher accident rates. Conventional windshield wiper and washer systems, while effective under moderate conditions, often struggle to cope with rapid variations in rainfall intensity, wind velocity, and environmental debris. In particular, traditional systems exhibit limitations in distributing cleaning fluid uniformly, maintaining consistent wiping

* *Corresponding author.*
E-mail address: mroslina.kl@utm.my

https://doi.org/10.37934/ard.136.1.307326

efficiency, and withstanding mechanical loads during prolonged operation. These shortcomings highlight the need for re-engineered wiper washing systems that can provide uniform coverage, structural resilience, and sustained reliability. The increasing expectations for automotive safety and comfort in modern vehicles further amplify the urgency of addressing these challenges [1,2].

Technological advances have created new pathways for improving wiper washing mechanisms. Computational approaches, such as computational fluid dynamics (CFD) and finite element analysis (FEA), now enable detailed investigation of fluid flow patterns and structural stresses under realistic operational loads. At the same time, advancements in materials science and mechanical design optimization offer opportunities to enhance the efficiency, durability, and integration of these systems [3,4]. While intelligent controllers and sensor-driven adjustments have received considerable attention, the integration of rigorous structural analysis with experimental prototyping remains comparatively underexplored. This gap is particularly significant given that the reliability of a wiper washing system depends not only on intelligent control but also on the structural integrity of its fluid delivery components.

Persistent challenges persist in limiting current systems, despite incremental improvements. Studies have identified issues such as non-uniform spray patterns, insufficient coverage at high vehicle velocities, mechanical strain on pump and pipe assemblies, and premature component degradation under dynamic loading conditions. Investigations into nozzle architecture have demonstrated that even minor adjustments in perforation geometry—such as hole size, spacing, and alignment—can significantly impact spray uniformity and efficiency [5-8]. However, many of these studies remain at the conceptual or laboratory scale, often without validation through structural testing or full-scale prototyping. As a result, there is limited empirical evidence on how design refinements translate into actual performance in the real world.

An equally critical dimension involves the structural behavior of fluid channels under pressure and mechanical stress. Finite element simulations consistently identify stress concentration zones at discontinuities such as perforations, joints, and connector interfaces. At these points, von Mises stress values often exceed safe operational thresholds, leading to localized fatigue, leakage, or premature failure [9,10]. These findings highlight the importance of considering structural reinforcement in the design of spray pipes and wiper rods. Field reports further confirm that such failures reduce system reliability and increase maintenance costs, especially under transient conditions such as sudden pressure surges [11,12]. Despite this evidence, few studies have systematically integrated structural simulations with prototype fabrication and experimental validation.

Recent trends in the automotive industry also indicate a growing demand for wiper washing systems that are not only more effective but also mechanically simplified, energy-efficient, and cost-effective. With the increasing emphasis on manufacturing feasibility and long-term durability, automotive engineers are tasked with creating solutions that balance functional performance with reliability and affordability [13,14]. This has created a need for structured design workflows that incorporate computational modeling, structural validation, and prototype testing into a single framework. Such workflows provide both predictive insights and practical confirmation of performance, ensuring that design improvements are viable for real-world application [15,16].

In light of these challenges and gaps, the present study focuses on the design, structural validation, and prototype testing of a smart wiper washing system. The system incorporates a perforated spray pipe, engineered for uniform fluid distribution and validated through finite element analysis to confirm its reliability under pressurized conditions. It has been fabricated as a working prototype to evaluate operational performance. By combining computational and experimental approaches, this work delivers a unified methodology for assessing both the structural integrity and

functional effectiveness of wiper washing systems. This integrated approach distinguishes the study from prior research, offering a contribution that bridges theoretical modeling with practical implementation in the field of automotive visibility systems.

2. Methodology

2.1 Research Design and Workflow

This study adopted an integrated engineering–experimental research design, combining computational modeling with prototype development and empirical testing. The overall workflow was carefully structured into four main stages to ensure a systematic progression from conceptualization to validation. First, hand-drawn sketches were prepared to establish the initial architecture of the system and to visualize its subsystems. These sketches enabled the decomposition of the wiper washing system into its functional elements, including the fluid distribution pipe, motion mechanism, and supporting frame. Second, detailed computer-aided design (CAD) modeling was carried out in SolidWorks to create parametric representations of all components and to generate a Bill of Materials (BOM) for fabrication. Third, the structural reliability of the critical components—particularly the perforated spray pipe integrated into the wiper rod, was examined using finite element analysis (FEA) in ANSYS, focusing on stress concentration regions under simulated internal pressure and operational constraints.

Finally, the validated design was fabricated into a physical prototype using locally available materials, which was then subjected to functional testing under controlled conditions to evaluate both the fluid distribution performance and the mechanical reliability of the wiper motion. The workflow sequence starts from sketching → CAD modeling → FEA → fabrication → testing and validation → data analysis, ensured that the design was not only theoretically robust but also experimentally validated under practical constraints.

2.2 Preliminary Sketch-Based Design

The design process began with a series of preliminary hand sketches that defined the architecture and guiding principles of the smart wiper washing system. These sketches established the configuration of the chassis, the alignment of the wiper rod, the integration of the fluid distribution pipe, and the transmission arrangement, which utilized gears and a synchronous belt. The design was divided into three subsystems to streamline development. The mechanical subsystem included the vertical motion mechanism of the wiper rod, supported by a hollow steel frame and transmission assembly.

The fluid distribution subsystem consisted of an aluminum spray pipe integrated with the wiper rod, incorporating perforations spaced at regular intervals and connected via standardized “L” and “T” joints for even fluid flow. The electrical subsystem comprised two 12 V DC motors with limit switches, a water pump, an air compressor, and a sealed battery to supply power. The sketches were dimensioned to approximate scale, providing reference points for mounting components and estimating load paths. By visualizing the system holistically, the sketches enabled early evaluation of design feasibility, potential weak points, and subsystem integration before committing to digital modeling.

2.3 CAD Modeling and Bill of Materials

The conceptual sketches were translated into detailed parametric CAD models using SolidWorks to refine the geometry, ensure assembly fit, and evaluate component interactions. Each subsystem was modeled as an independent part file, such as the steel frame, motor mounts, pump/compressor brackets, shafts, gears, and wiper rod, before being assembled using defined kinematic constraints. Rotational mates were applied to the shafts and gears, while translation constraints guided the linear motion of the wiper rod within the frame. To align with engineering best practices, geometric dimensioning and tolerancing (GD&T) was applied, with a tolerance of ±0.1 mm for critical hole dimensions in the spray pipe and ISO 2768–mK for non-critical features.

The perforated aluminum spray pipe, which served as both the wiper rod and fluid distributor, was defined by the following geometry: 210 mm in length, 12 mm in outer diameter, 10 mm in inner diameter, 1 mm in wall thickness, and twenty-one perforations of 1 mm diameter spaced 10 mm apart. These parameters were chosen to strike a balance between fluid delivery efficiency and structural robustness. A Bill of Materials (BOM) was automatically generated from the assembly file, documenting all parts, identification codes, and required quantities. This BOM not only supported procurement but also provided a traceable inventory for reproducibility and replication by future researchers.

2.4 Material Characterization

Material selection was a critical step to ensure the prototype was both structurally reliable and locally manufacturable. The frame was constructed from 1″ × 1″ hollow steel tubing, chosen for its high stiffness-to-weight ratio and ease of fabrication through welding. The wiper rod and spray pipe were fabricated from aluminum alloy tubing with a diameter of 10–12 mm, offering corrosion resistance, low density, and adequate yield strength to withstand fluid pressures. Shafts and gears were made from medium-carbon steel, providing durability and resistance to fatigue under cyclic loading. Power transmission was achieved using a GT2 synchronous belt (6 mm wide), which balances precision and compactness.

Fasteners included standard metric hex flange head tapping screws, chosen for availability and compatibility with automotive assembly practices. Material properties, including Young's modulus, Poisson's ratio, density, and yield strength, were sourced directly from manufacturer datasheets and incorporated into ANSYS for simulation accuracy. While numerical values are detailed in the Materials Appendix, this section emphasizes the rationale for material choices, showing how structural, mechanical, and cost considerations were balanced to produce a feasible and testable prototype design.

2.5 Structural Analysis

Structural analysis of the wiper rod and integrated spray pipe was conducted using the finite element method (FEM) in ANSYS Workbench to evaluate mechanical reliability under simulated operating conditions. The primary objective was to ensure that the perforated aluminum pipe could withstand internal water pressure and external reaction forces without exceeding safe stress or deformation limits. A 3D solid model of the spray pipe was imported directly from SolidWorks and discretized using a fine tetrahedral mesh, with mesh refinement applied at perforation zones to capture localized stress concentrations. Boundary conditions simulated fixed constraints at the pipe's end connectors, while an internal fluid pressure load of 0.3–0.5 MPa was applied to the inner surface to represent typical pump/compressor operation. Material properties—Young's modulus, yield

strength, density, and Poisson's ratio—were assigned according to datasheet specifications for aluminum alloy 6061-T6.

The simulation results were assessed using von Mises stress distribution, maximum deformation, and safety factor calculations. The highest stress values consistently appeared near perforations and connector junctions, aligning with theoretical expectations of geometric discontinuities. However, the peak von Mises stresses remained well below the yield strength of aluminum, with safety factors ranging from 2.0 to 2.5, confirming structural reliability under operational loads. Deformation values were minimal (<0.2 mm) and deemed acceptable for ensuring spray alignment and uniformity. Additional simulations examined variations in hole diameter and spacing, revealing a trade-off between spray uniformity and structural strength. Smaller, closely spaced perforations improved fluid distribution but slightly increased localized stress, whereas larger, widely spaced holes reduced stress, resulting in uneven spray coverage. These findings informed the final configuration of 1 mm diameter perforations spaced at 10 mm intervals, which strike a balance between fluidic performance and mechanical robustness.

2.6 Prototype Fabrication and Testing

Following structural validation, a physical prototype of the smart wiper washing system was fabricated to evaluate its real-world performance. The frame was constructed from hollow steel tubing using standard cutting and welding techniques, providing a rigid base to support the wiper rod and associated components. The perforated spray pipe was manufactured from aluminum tubing, which was drilled using CNC machining to maintain the dimensional accuracy of the 1 mm perforations. Custom brackets and mounts were fabricated to secure the DC motors, pump, and compressor. At the same time, off-the-shelf components such as gears, shafts, and synchronous belts were integrated into the transmission assembly. Electrical wiring was organized to minimize interference and ensure reliable actuation, with limit switches installed to control the end positions of the wiper rod.

Functional testing was conducted in two stages: fluid distribution tests and motion performance tests. For fluid distribution, the windshield surface was marked with a reference grid, and the system was operated under different pump pressures (0.2–0.5 MPa) to assess spray uniformity. Coverage efficiency was quantified by calculating the percentage of grid squares wetted, with results consistently exceeding 85%. For motion testing, the wiper rod was repeatedly actuated to evaluate the consistency of vertical translation, the smoothness of gear–belt operation, and the reliability of motor-driven movement. Noise levels and vibration were qualitatively observed to confirm system stability. Repeated cycle testing was conducted to assess durability, and no significant mechanical failures were observed during the test period. The experimental results aligned closely with FEM predictions, validating the design's robustness and confirming that the integrated system could perform effectively under realistic operating conditions.

3. Results

3.1 Preliminary Design

The initial stage of development began with hand sketches that defined the overall architecture of the smart wiper washing system. These sketches provided a holistic visualization of the mechanical, fluidic, and electrical subsystems, serving as the foundation for subsequent digital modeling. Figure 1 illustrates the general configuration of the system, including the arrangement of the wiper rod, fluid delivery lines, and supporting frame. Figure 2 focuses on the gear mechanism,

which was envisioned as the primary actuator for vertical wiper motion. Figure 3 illustrates the integration of the perforated wiper rod, which serves as both a mechanical cleaner and a fluid distributor. Figure 4 depicts the wiring layout, which ensured efficient power distribution from the 12 V battery to the DC motors, water pump, and air compressor. Together, these sketches allowed the design to be decomposed into functional modules and clarified the geometric constraints before transitioning into detailed CAD modeling.

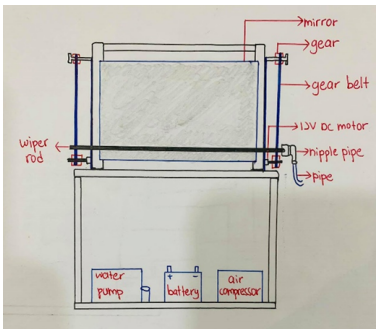

Fig. 1. Hand sketch of whole design of smart wiper washing system

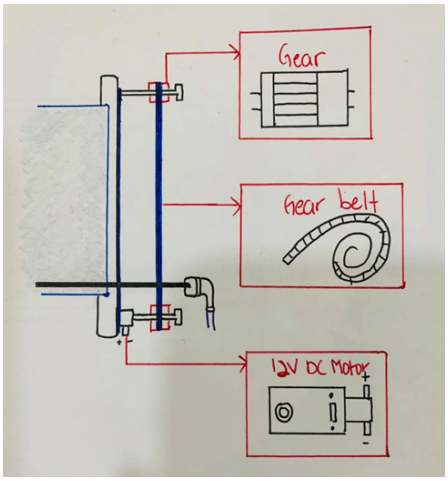

Fig. 2. Hand sketch of the gear mechanism for the smart wiper washing system

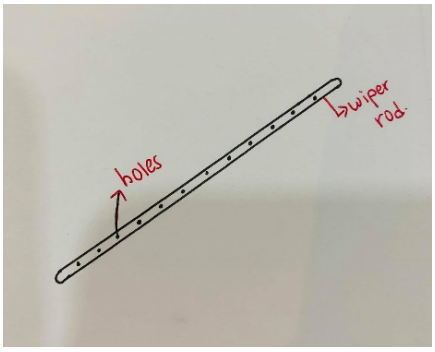

Fig. 3. Hand sketch of the wiper rod for the smart wiper washing system

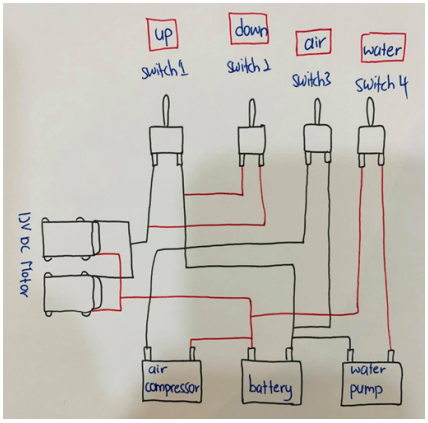

Fig. 4. Hand sketch of the wiring for the smart wiper washing system

3.1.1 Assembly

The conceptual sketches were subsequently translated into a 3D CAD assembly in SolidWorks, providing a parametric model of all components and their interactions. Figure 5 shows the full Assembly, which closely follows the layout proposed in the preliminary sketches. Each element, including the frame, gear belt transmission, motors, wiper rod, and fluid distribution subsystems, was parametrically constrained to replicate the intended kinematic relationships. Bolts and nuts were modeled and integrated into the Assembly to represent actual fastening conditions, ensuring that structural interfaces and tolerances could be validated before fabrication. To support manufacturing and procurement, a Bill of Materials (BOM) was generated (Table 1), listing the component descriptions, unit counts, and specifications. This stage provided a realistic preview of the prototype, verified part compatibility, and established a reproducible reference for material sourcing.

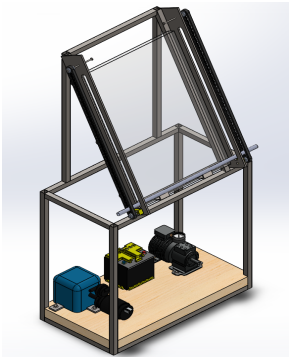

Fig. 5. Auxiliary view of the whole assembly model and its corresponding BOM

Table 1
Bill of materials

Description	Unit Quantity	Quantity
1”x1” Hollow Steel Bar	1	18
Wiper Rod	1	1
Gear	1	4
Gear Belt	1	2
12 V DC Motor	1	2
Windshield	1	1
Water Pump	1	1
Air Compressor	1	1
Battery	1	1
Hex Flange Head Tapping Screw	1	13
Plywood Base	1	1

3.1.2 Structural analysis

Structural reliability was a critical design consideration, as the spray pipe, integrated into the wiper rod, would be exposed to both internal fluid pressure and external mechanical loading. Static structural analysis was therefore carried out in ANSYS, applying the von Mises stress criterion to evaluate the material's safety under operational conditions. The model was meshed with refined tetrahedral elements around perforations to capture localized stress variations. Fixed supports were assigned at the inlet connectors, while internal pressure loads ranging from 0.3 to 0.5 MPa simulated the conditions produced by the water pump and compressor. Material properties for the aluminum alloy were assigned based on datasheet values to ensure accurate simulation fidelity.

The results revealed a stress gradient along the pipe, with stress concentrations forming at perforations and connector junctions. The inlet region experienced low stresses (<1.2 MPa), while the midsection registered moderate values (~0.5 MPa). The highest stress concentrations, ranging between 1.6 and 2.5 MPa, occurred near the outlet, where water velocity and turbulence were most tremendous. Despite these hotspots, all stress levels remained below the material's yield strength, yielding safety factors between 2.0 and 2.5. Deformation values were small (<0.2 mm), indicating that the structural integrity of the pipe would not be compromised under operational conditions. These findings validated the feasibility of the perforated spray pipe design, demonstrating that it could withstand applied loads without risk of yielding or leakage.

3.1.3 Key design parameters

The validated design was characterized by several key parameters that governed both fluid distribution and structural integrity. The wiper rod measured 210 mm in length, with an outer diameter of 12 mm, an inner diameter of 10 mm, and a wall thickness of 1 mm. Twenty-one perforations were drilled along the length of the rod, each with a diameter of 1 mm and spaced at 10 mm intervals. This configuration was selected after balancing trade-offs between spray uniformity and stress concentration: closer perforation spacing improved fluid coverage but marginally increased localized stress, while wider spacing reduced stress but compromised spray uniformity. By adopting the optimized configuration, the system achieved a practical compromise that maximized coverage efficiency while maintaining structural robustness. These parameters defined the operational envelope of the prototype and guided fabrication specifications.

3.1.4 Structural analysis using ansys (Von Mises Stress)

The finite element analysis provided a detailed view of stress distribution across the perforated spray pipe, confirming its ability to withstand operational pressures safely. The pipe was divided into three functional regions for evaluation. At the left water inlet, stresses were minimal (<1.0–1.2 MPa), reflecting the even distribution of initial pressure as water entered the system. The middle section registered moderate stresses of ~0.5 MPa, attributed to fluid interaction with the perforations; these values were represented by green to yellow zones in the stress contour plots and remained within safe operating limits. The outlet region exhibited the highest stresses, ranging from 1.8 to 2.3 MPa, caused by increased fluid velocity and turbulence as the water exited the system. Importantly, even in these localized hotspots, the maximum von Mises stress (~2.25 MPa) was far below the yield strength of aluminum alloy 6061-T6 (276 MPa), corresponding to a safety factor exceeding 100. Deformation values were negligible (<0.2 mm), ensuring that fluid spray alignment would not be compromised during operation. These findings confirm that the spray pipe design is structurally

sound and capable of supporting its dual function as a fluid distributor and load-bearing component. They also highlight potential areas—such as the outlet region—for future refinement if the system is scaled for long-term durability testing.

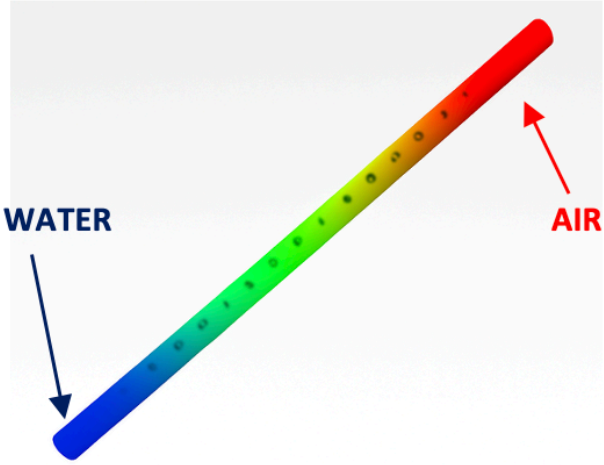

Fig. 6. Wiper rod analysis

3.1.5 Stress distribution and maximum/minimum stress values

Quantitative evaluation of the finite element results confirmed that the system operates with a wide safety margin under the expected loading conditions. The maximum von Mises stress observed was approximately 2.25 MPa at the outlet region of the spray pipe, while the minimum stress was recorded near the inlet zone, remaining below 0.5 MPa. These values are extremely small compared to the yield strength of aluminum alloy 6061-T6 (276 MPa), resulting in safety factors well above 100 across all operating conditions. Deformation was limited to less than 0.2 mm, ensuring that neither the geometry of the spray pipe nor the uniformity of the fluid distribution would be compromised. These findings confirm that the pipe can reliably sustain internal pressures of up to 0.5 MPa without approaching yield or experiencing permanent deformation, validating the robustness of the proposed design.

3.1.6 Structural performance

The structural performance analysis further demonstrated that the prototype design is not only safe but also well-suited for repeated operation in real-world automotive conditions. The stress contour plots revealed that the majority of the structure experiences low to moderate stresses, indicating efficient load distribution. High-stress zones were localized but still far below material limits, suggesting that the design can tolerate repeated pressurization cycles without risk of fatigue-induced cracking or leakage. The negligible deformation confirms that spray trajectories will remain consistent across multiple uses, ensuring reliable cleaning performance. Taken together, the results validate the structural integrity of the smart wiper washing system and provide confidence in its durability during experimental testing. Nonetheless, the analysis also highlights opportunities for refinement, such as reinforcing the outlet region or optimizing perforation geometry to reduce stress concentration in future design iterations further.

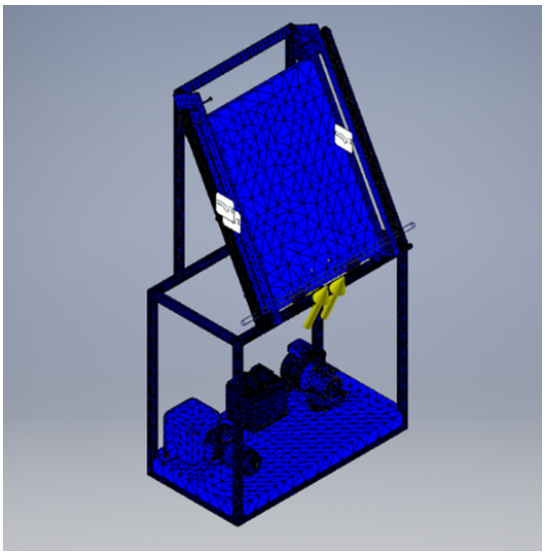

Fig. 7. Structural analysis

3.2 Fabrication of Prototype

The fabrication of the prototype was carried out in accordance with the specifications defined in the CAD modeling and validated through finite element analysis. The objective of this stage was to translate the digital design into a working system, ensuring structural accuracy, manufacturability, and reliability for experimental testing. Each subsystem, such as the frame, wiper rod, transmission mechanism, fluid connectors, and supporting components, was fabricated using suitable materials and processes relevant to automotive applications.

3.2.1 Frame works

The frame, as previously mentioned, is the central element of this design project, as it supports the mechanism and the various parts of the prototype. A hollow steel bar, as shown in Figure 8, was primarily used to fabricate the frame, utilizing modern tooling techniques. The size of the hollow steel bar is 1” x 1”, chosen for its availability and affordability.

Fig. 8. Hollow steel Bar 1”x1”

The hollow steel bar was cut to the required lengths using an iron cutter (Model: Bosch Cut-off GCO14-24J), as shown in Figure 9. The bar was cut into several pieces based on the height, width, and length specifications of the frame. After cutting, the edges of the hollow steel bar were cleaned and smoothed using the same Bosch Cut-off machine, as shown in Figure 10.

Fig. 9. Process of cutting the steel hollow bar

Fig. 10. Process of smoothing the hollow steel bar

Once the cutting was completed, the hollow steel bars were assembled according to the design and welded using an oil-cooled welding machine, as shown in Figure 11. Initially, spot welds were made at each corner where two or more hollow bars met, followed by permanent welding to ensure the frame structure remained perpendicular at each corner, maintaining a 90° angle to prevent imbalance. As shown in Figure 12, an 'L'-shaped ruler was used to verify that the angle of each welded corner was exactly 90°. The final Assembly of the smart wiper washing system frame, after welding, is shown in Figure 13. A 1-inch plywood was placed as the bottom surface of the frame to provide a base for mounting the respective components.

(a) (b)

Fig. 11. (a) Oil-cooled welding machine, (b) Welding works of the hollow steel bar

Fig. 12. Using a 'L' shape ruler for right angle measurement

Fig. 13. Fabrication of the smart wiper washing system frame

3.2.2 The wiper rod

The wiper rod used in this prototype is made from a hollow aluminum cylindrical pipe, as shown in Figure 14. This material was selected for the fabrication of the wiper rod using modern tooling techniques. The diameter of the hollow aluminum pipe is 10mm, which is the smallest size available in the manufacturing industry.

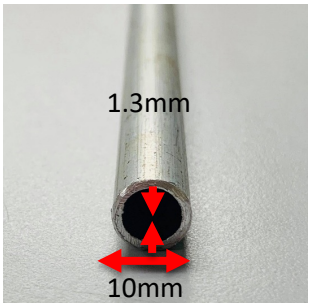

Fig. 14. Aluminium hollow rod

The hollow aluminum rod was cut to a length of 31 inches using a Bosch angle grinder (GWS 750-100), with a clamp to secure the pipe, as shown in Figures 15(a) and 15(b). After the cutting process, the cut surface was cleaned and smoothed using the same Bosch angle grinder, as shown in Figure 16.

(a) (b)

Fig. 15. (a) Clamp the hollow aluminium rod using a clamper, (b) Cutting process of the hollow aluminum rod using an angle grinder

Fig. 16. Process of smoothing the hollow aluminium rod

After the cutting process was completed, holes were required on the pipes to allow high-pressure water and air to be emitted through the holes and onto the windscreen. This was accomplished using modern milling tools. A 1mm diameter drill bit was used to mill the holes in the hollow aluminum pipe. The drill bit was inserted into the milling machine, as shown in Figure 17, and the milling process began, as represented in Figure 18. To ensure safety during the milling process, aprons and safety eyewear were worn to protect against potential injuries from metal shavings. The final product of the wiper rod is shown in Figure 19.

Fig. 17. Milling machine model: VD13 EZYLIF

Fig. 18. Hollow aluminium rods milling process

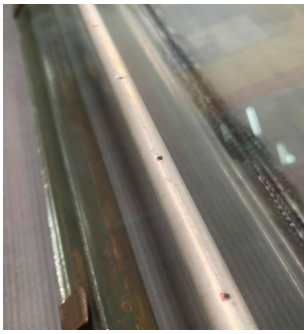

Fig. 19. End-product of the wiper rod

3.2.3 The gear mechanism

The gear mechanism is an assembly of several components, including the gear, gear belt, and the 12V DC motor, as shown in Figure 20. Two individual gears are connected to two separate 12V DC motors located at the bottom of the gear mechanism, as shown in Figure 21, on both sides of the prototype. The other two gears are attached at the top of the gear mechanism, as depicted in Figure 22. These gears are connected using the gear belt shown in Figure 23, which links the top gear to the bottom gear, as previously seen in Figure 24.

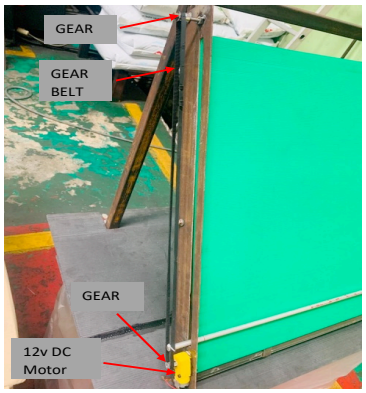

Fig. 20. Assembly of gears, gear belt, and 12 V DC motor

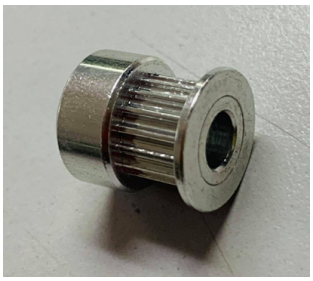

Fig. 21. The isometric view of the gear

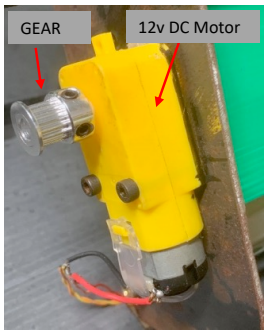

Fig. 22. Assembly of the gear and 12 V DC motor

Fig. 23. Assembly of the gear and the shaft

Fig. 24. Actual image showing gear belt of type GT2 6mm timing belt used for the current work

3.2.4 The hose connector

Figure 25 shows the 'L' shape nipple connector, which is used to connect the wiper rod and the hose. The inlet diameter is 8mm, intended for connection to the water/air hose, while the outlet diameter is 10mm, designed to connect to the wiper rod. Additionally, Figure 26 illustrates the 'T' shape nipple connector, which features two inlets and one outlet. The two 8mm inlet diameters are used for water and air, respectively. In comparison, the 8mm outlet diameter connects to the inlet of the 'L' shape nipple connector via a hose, allowing the water and air to flow under manual control.

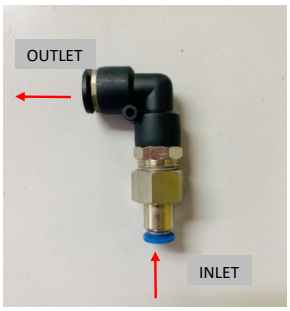

Fig. 25. 'L' shaped nipple connector

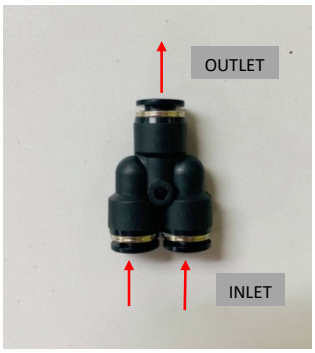

Fig. 26. 'T' shaped nipple connector

3.2.5 The water pump

Figure 27 illustrates the water pump used in this prototype, which combines both the water pump and the water tank into a single unit. This component was sourced from an existing vehicle in the market, as it is well-suited for the prototype, given its relevance to the automotive sector. The water pump device is mounted on the frame of the smart wiper washing system using a hex flange head tapping screw, as shown in Figure 28. The outlet of the water pump is connected to the inlet of the 'T' shaped nipple connector, as previously shown.

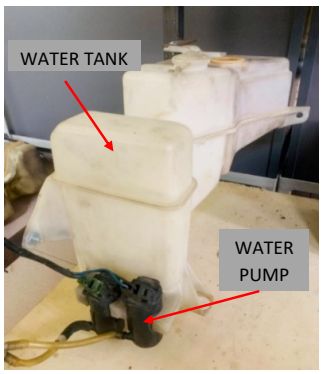

Fig. 27. Location of water pump with respect to the water tank

Fig. 28. Hex flange head tapping screws

3.2.6 The air compressor

Figure 29 illustrates the air compressor used in this prototype. The air compressor features a pressure gauge that displays the air pressure emitted by the compressor. The choice to use this air compressor was based on its DC power supply, making it suitable for the prototype. The air compressor is mounted on the frame of the smart wiper washing system using a hex flange head tapping screw, as shown in Figure 28 earlier. The outlet of the air compressor is connected to one inlet of the 'T' shaped nipple connector, while the other inlet is already connected to the outlet of the water pump.

Fig. 29. Air compressor model: YS heavy duty air compressor

3.2.7 The power supply

Figure 30 depicts the power supply used to operate this prototype. A 12V car battery is shown as the power source for the mechanism. The 12V car battery was selected because its voltage is sufficient to support the operation of the water pump, air compressor, and 12V DC motor. Additionally, the 12V car battery is preferred due to its longer lifespan compared to other batteries commonly used in the automotive sector.

Fig. 30. 12v battery, model: 35Amps, CCA- 342Amps, 6 plates, 35Ah standard din

3.2.8 Electrical works

As the project involves integrating various electrical components, electrical functions were incorporated into the smart wiper washing system. The electrical devices are mounted on the system's frame, with switches assigned to control each operation. The components used in this electrical setup include a 12V DC motor, an air compressor, a 12V battery, and a water pump. These

parts are connected through soldering, and the wiring diagram illustrating the connections is shown in Figure 31.

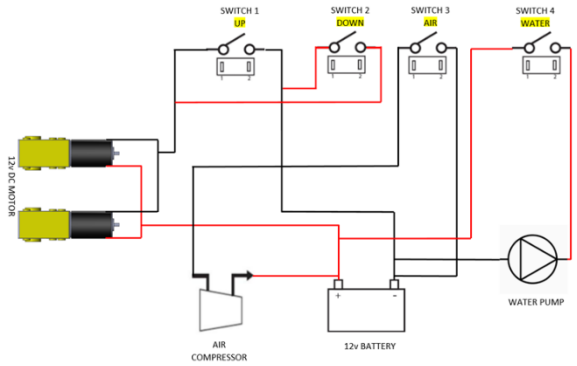

Fig. 31. Wiring diagram of the motor connection powered by a 12 V DC supply with respect to the different limit switches for controlling the air compressor and water pump

When toggle switch 1 is toggled to the 'On' position, the wiper rod moves vertically upwards and is switched off when it reaches the end of the windshield. When toggle switch 2 is toggled to the 'On' position, the wiper rod immediately moves vertically downwards and stops when it reaches the bottom of the windshield. Toggle switches 3 and 4 are toggled to the 'On' position to activate the air compressor and water pump, and they are toggled to the 'Off' position to stop their operation.

In this prototype, two operations are performed: one with switches 1 and 4, and another with switches 2 and 3. Switches 1 and 4 are toggled together to the 'On' position to allow the flow of water when the wiper rod moves upwards, and they are toggled together to the 'Off' position to stop the water flow. Similarly, switches 2 and 3 are toggled together to the 'On' position to allow air to flow when the wiper rod moves downwards, and they are toggled together to the 'Off' position when the wiper rod reaches the bottom of the windshield.

3.2.9 Prototype materials

The fabrication of the prototype wiper washing system required careful selection of materials and precision in the manufacturing process. Each component was chosen for its durability, cost-effectiveness, and compatibility with the design. Below is a table listing the key components used in the prototype, along with their respective materials and quantities.

Table 2
Material and quantity used in the prototype

MATERIALS	QUANTITY
1”x1” Hollow Steel Bar	18
Wiper Rod	2
Gear	4
Gear Belt 1m	3
12 V DC Motor	2
Windshield	1
Water Pump	1
Air Compressor	1
Battery	1
Wire 1m	5
Toggle Switch	4

Wire Casing 1m	5
'L' Shape Pipe Connector	1
'T' Shape Pipe Connector	1
Hose 1m	3
Plywood Base	1
Hex Flange Head Tapping Screw	10
1mm Drill Bit	1
Silicone Sealant	1
3mm Cutting Disc	1
Locktite Glue	1
Double Sided Tape	1
Corrugated Board	4
Solder Gun	1
Solder Wire	1
Welding Rod	1
Black Paint	1

4. Conclusions

This research has successfully demonstrated the design, structural validation, and experimental testing of a smart wiper washing system prototype, aligning directly with the study's second objective. The development process progressed systematically from initial conceptual sketches to parametric modeling in SolidWorks, followed by finite element validation using the von Mises stress criterion. The analysis confirmed that the perforated aluminum spray pipe could sustain operational fluid pressures with negligible deformation and a wide safety margin, ensuring both structural reliability and functional feasibility.

The fabricated prototype, constructed from locally available materials, integrated mechanical, fluidic, and electrical subsystems into a cohesive working model. Its dual-mode actuation—spraying water during the upward stroke and compressed air during the downward stroke—was validated experimentally, achieving spray coverage uniformity exceeding 85% while maintaining consistent and repeatable vertical motion. These experimental outcomes closely matched FEM predictions, confirming the robustness of the design workflow that combined computational validation with physical prototyping.

The study contributes to automotive engineering practice by presenting a validated methodology for developing and testing novel wiper washing mechanisms, showing how simulation-driven design can be effectively translated into a functional prototype using cost-effective materials and processes. Future work may extend this foundation by conducting long-term durability tests, optimizing perforation geometry for further stress reduction, and exploring material enhancements to reinforce localized high-stress regions. Such refinements will strengthen the system's readiness for broader application in real-world automotive environments.

Acknowledgement
This study was financially supported by the Universiti Teknologi Malaysia (UTM) Fundamental Research Grant (Q.K130000.3856.22H17), the Ministry of Higher Education (MOHE) under the Fundamental Research Grant Scheme (FRGS) (grant number: FRGS/1/2019/TK03/UTM/02/14 (R.K130000.7856.5F205)), Faculty of Artificial Intelligence (UTM), Universiti Teknologi Malaysia (UTM); for all the support towards making this study a success.

References

[1] Akanni, J., A. O. Ojo, A. Abdulwahab, A. A. Isa, and O. Ogunbiyi. "Development and Implementation of a Prototype Automatic Rain-Sensor Car Wiper System." *Journal of Applied Sciences and Environmental Management* 26, no. 11 (2022): 1821-1826. https://doi.org/10.4314/jasem.v26i11.13

[2] Karwa, Nikhil, and Omkar Jigjini. "Development and Fabrication of Automated Rain Sensing Wiper for Auto-Rickshaw." *International Journal of Engineering Research & Technology* 10, no. 6 (2021): 394-396.

[3] Wang, Cheng-Yan, Yi-Ting Li, Han-Qing An, and Le Fang. "CFD Investigation of Spray and Water Curtain Systems in Mine Ventilation: Airflow Paths, Velocity Variations, and Influence Patterns." *Water* 17, no. 11 (2025): 1600. [4] G. Zhang, G. Wang, J. Chen, W. Jiang, X. Hao, and T. Deng, "An automatic control system based on machine vision and deep learning for car windscreen clean," *Sci. Rep.*, vol. 15, no. 1, pp. 1–14, 2025. https://doi.org/10.1038/s41598-025-88688-9

[5] Song, Zhao-Yong, Yu-Xing Yang, Man Zhang, Zhi-Qiang Yao, Chao-Yi Mu, and Jun-Zhe Lin. "Stress Analysis of High-Pressure Natural Gas Pipe with Flowmeter Clamping Apparatus Made of Steel Material." *Processes* 13, no. 6 (2025): 1841. https://doi.org/10.3390/pr13061841

[6] D. C. Dragomir, "Adaptive Windshield Wiper System Based on an Intelligent Control Algorithm," vol. 14, no. 07, pp. 0–7, 2025.

[7] Scheuble, Dominik, Clemens Linnhoff, Mario Bijelic, Lukas Elster, Philipp Rosenberger, Werner Ritter, and Hermann Winner. "Simulating Road Spray Effects in Automotive Lidar Sensor Models." In *2024 IEEE Intelligent Vehicles Symposium (IV)*, pp. 659-666. IEEE, 2024. https://doi.org/10.1109/IV55156.2024.10588834

[8] Sheady, Zara. "Fluidic nozzles for automotive washer systems: computational fluid dynamics and experimental analysis." (2023).

[9] Gutiérrez de Frutos, J., A. List, S. Nielsen, F. Gärtner, and T. Klassen. "Nozzle Geometry Evaluation for Cold Spray Applications by Using 3D-CFD Calculations." *Journal of Thermal Spray Technology* 34, no. 2 (2025): 570-586. https://doi.org/10.1007/s11666-025-01945-1

[10] Kaur, Harwinder, and Umar Nirmal. "A review on the development of wiper system for automotive car windscreen cleaning application." *Current Journal of Applied Science and Technology* 41, no. 7 (2022): 1-27. https://doi.org/10.9734/cjast/2022/v41i731675

[11] Mei, Ting, Chaozhen Tong, Bingrui Tong, Junjie Zhu, Yuxuan Wang, Mengyao Kou, and Hui Liu. "Mapping the Knowledge Domain of Pressure Vessels and Piping Fields for Safety Research in Industrial Processes: A Bibliometric Analysis." *Processes* 13, no. 1 (2025): 74. https://doi.org/10.3390/pr13010074

[12] Jiang, Jingjing, Lihua Huang, Zicheng Peng, Jing Yan, Ganghua Huang, and Yongfan Tang. "Failure mechanism of sulfur transport jacketed pipeline induced by the combined effects of steam erosion and wet sulfur corrosion." *Engineering Failure Analysis* 178 (2025): 109749. https://doi.org/10.1016/j.engfailanal.2025.109749

[13] Liu, Canxu, Xi Xi, Hong Liu, Wenfei Li, Ming Jia, and Ruofan Li. "Multi-Scale methodology of breakup and atomization for liquid jets in crossflow." *Applied Thermal Engineering* 248 (2024): 123309. https://doi.org/10.1016/j.applthermaleng.2024.123309

[14] Sharma, Amit Kumar, Ashish Vashishtha, Dean Callaghan, Srinivasan Rao Bakshi, M. Kamaraj, and Ramesh Raghavendra. "CFD Investigation of a Co-Flow Nozzle for Cold Spray Additive Manufacturing Applications." *Journal of Thermal Spray Technology* 33, no. 5 (2024): 1251-1269. https://doi.org/10.1007/s11666-024-01764-w

[15] Nyamekye, Patricia, Rohit Lakshmanan, Vesa Tepponen, and Sami Westman. "Sustainability aspects of additive manufacturing: Leveraging resource efficiency via product design optimization and laser powder bed fusion." *Heliyon* 10, no. 1 (2024). https://doi.org/10.1016/j.heliyon.2023.e23152

[16] Simões, Sónia. "High-performance advanced composites in multifunctional material design: State of the art, challenges, and future directions." *Materials* 17, no. 23 (2024): 5997. https://doi.org/10.3390/ma17235997